Наносистеми, наноматеріали, нанотехнології
Nanosistemi, Nanomateriali, Nanotehnologii
2021, т. 19, № 4, сс. 841–853

PACS numbers: 71.15.Mb, 71.20.Rv, 76.60.-k, 78.30.-j, 78.40.-q, 78.67.Sc, 82.35.Np

Exploring the Optical, Electronic, and Spectroscopic Properties of Yttrium Oxide Doped PVA/PEG Blend for Low Cost and Lightweight Electronics Applications

Hind Ahmed and Ahmed Hashim

College of Education for Pure Sciences,
Department of Physics,
University of Babylon,
Hillah, Iraq

This paper is focused on the structural, electronic, and spectroscopic properties of PVA–PEG–Yttrium oxide blend (64 atoms), by using density functional theory (DFT) at the B3LYP level with 6-311G basis set. All calculations are performed with Gaussian 09 program and Gaussian view 5.0.8 program. The geometric properties include improving geometric optimization of bonds and angles. As the electronic properties, there are considered such as ionization potential, electron affinity, chemical hardness, chemical softness, electronegativity, total energy, cohesive energy, energy gap, electrophilicity, and density of states (DOS). In addition, the spectral properties are involved (IR, Raman, NMR, and UV-Visible). The results show that the 6-311G basis sets are efficient and strongly suggested for heavy metals and give good relaxation for the structure. The results state that the yttrium oxide has the low LUMO–HOMO energy gap, and it gives more biological activity ratios. The obtained results indicate that the PVA–PEG–Yttrium oxide blend can be used in different fields for electronics and photonics applications.

Цю статтю зосереджено на структурних, електронних і спектроскопічних властивостях суміші полівініловий спирт (ПВС)/поліетиленгліколь (ПЕГ) із домішкою Y_2O_3 (64 атоми) із використанням теорії функціоналу густини (ТФГ) на рівні B3LYP із базисним набором 6-311G. Всі розрахунки виконуються за допомогою програми Gaussian 09 і програми Gaussian View 5.0.8. Геометричні властивості включають поліпшення геометричної оптимізації зв'язків і кутів. В якості електронних властивостей розглядаються: потенціял йонізації, спорідненість електронів, хемічна цупкість, хемічна м'якість, електронеґативність, повна енергія, когезійна енергія, енергетична щілина, електрофільність і густина електронних станів. Крім того, задіяні спектральні властивості (ІЧ, Раманові, ЯМР і у видимому й ультрафіолетовому діяпазонах світла).

Результати показують, що базисні набори 6-311G є ефективними та настійно пропонуються для важких металів і дають хорошу релаксацію для структури. Результати показують, що оксид Ітрію має низьку енергетичну щілину LUMO–HOMO, і він дає більше коефіцієнтів біологічної активности. Одержані результати свідчать про те, що суміш оксиду ПВС–ПЕГ–оксид Ітрію може використовуватися в різних областях для застосування електроніки та фотоніки.

Key words: PVA/PEG blend, Y_2O_3 admixture, NMR, spectral properties, DFT, 6-311G basis, electronics.

Ключові слова: суміш полівініловий спирт/поліетиленгліколь, домішка Y_2O_3, ЯМР, спектральні властивості, ТФГ, 6-311G-базис, електроніка.

(Received 19 January, 2021; in revised form, 22 January, 2021)

1. INTRODUCTION

Yttrium oxide is promising for chemical catalysis devices and for optoelectronics. It is used for biological imaging applications [1]. Yttrium oxides are the two most important ceramic materials, which have wide technological applications ranging from electronics, optics, and mechanical engineering to catalyst support [2]. Yttrium and yttrium oxide has been studied both experimentally and theoretically owing to their possible applications [3]. Nanocomposites are a new-fangled class of materials made with nanosize fillers. Nanosize inorganic particles mixed with organic polymer are called organic–inorganic hybrids [4]. Polymer matrixes reinforced with nanosize phase (nanofillers) such as nanoparticles, nanotubes, nanosheets, and nanofibers, *etc.*, called polymer nanocomposites, have the physical properties of these composites mainly depending on the contact of polymer molecules with nanofillers [5]. Transition metal oxides are known for their great change in effects of chemical and physical properties. Several of those materials undergo phase transitions with interesting structural, electronic, and magnetic behaviours [6]. In nature, there is a water-soluble and easily degradable material; it is polyvinyl alcohol (PVA). Hence, it acts as an ecofriendly polymer [7]. It may be applied naturally to create thin films with metal oxide. Strong absorption properties are revealed for PVA polymer in the range 300 to 500 nm in the ultraviolet (UV) spectra [8]. There are many studies on some properties of doped polymers like structural, optical, electrical, and electronic properties [9–36]. DFT is proven as very successful in calculating the structural properties of condensed systems and electronic properties of simple metals [37]. That distinguishes the method of density functional theory is choosing the shape of function to compute the

energy of bonding and exchange [38].

2. THEORETICAL PART

The total energy for a system is the sum of total kinetic and potential energies at the optimized structure such that the total energy of the molecule must be at the lowest value because the molecule is at the equilibrium point. This means the resultant of the effective forces is zero. Cohesive energy is defined as 'the energy necessary to detaching the condensed material into separated atoms'. The relation (1) is used to compute the cohesive energy, which means 'the difference between energy per atom of the bulk material at equilibrium and energy of a free atom in its ground state' [39]:

$$E_{\text{coh}} = \left(\frac{E_{tot}}{n} \right) - E_{free} - E_0 , \tag{1}$$

where E_{tot} is the total energy, E_{free} is the free-atoms' energy, n is number of atoms, E_0 is the vibrational energy of ground states (zero-point).

The HOMO (the molecular orbitals of highest energy that is occupied by electrons) and LUMO (the molecular orbitals of lowest energy that is not occupied by electrons) are main orbitals in calculations of such properties as the molecular interaction and the ability of molecule to absorb a light. According to Koopmans' theorem, the band gap is given as follows [40]:

$$E_g = E_{\text{LUMO}} - E_{\text{HOMO}}. \tag{2}$$

For the molecule, there is the magnitude of energy needed to eliminate the electron from atom or isolated molecule and identified as energy difference between the positive charge energy $E_{(+)}$ and neutral one $E_{(n)}$ by the following relation:

$$IP = E_{(+)} - E_{(n)}. \tag{3}$$

When electrons are additional to neutral atoms to form a negative ion, it is stated as 'the energy difference between the neutral energy $E_{(n)}$ and the negative charge energy $E_{(-)}$' by the following relation:

$$EA = E_{(n)} - E_{(-)}. \tag{4}$$

In molecular orbital (MO) theory within the limitation of Koopmans' theorem, the orbital energies of the frontier orbitals are given as follow:

$$IP = -E_{\mathrm{HOMO}}, \tag{5}$$

$$EA = -E_{\mathrm{LUMO}}. \tag{6}$$

The chemical hardness (η) is a measure of the range of resistance to the transfer of charges [40, 41]. It is theoretically defined as 'the second derivative of electron energy in relation to the number of electrons N' for a constant external potential $V(r)$ [41]:

$$\eta = \frac{1}{2}\left[\frac{\partial^2 E}{\partial N^2}\right]_V = \frac{1}{2}\left[\frac{\partial \mu}{\partial N}\right]_V = -\frac{1}{2}\left[\frac{\partial X}{\partial N}\right]_V. \tag{7}$$

Finite-difference approximation for the chemical hardness gives:

$$\eta = \frac{IP - EA}{2}. \tag{8}$$

The chemical softness, S, is a 'property of molecules that measures the degree of chemical reactivity'. It is the converse of the chemical hardness (η) [42]:

$$S = \frac{1}{2\eta}\left[\frac{\partial^2 N}{\partial E^2}\right]_V = \left[\frac{\partial N}{\partial \mu}\right]_V. \tag{9}$$

The fundamental variation principle within the density functional theory is the electron chemical potential, where the reactivity indicator is related to how the electron energy E of molecules is changed with changing the number of electrons (N) and the external potential. Chemical potential μ is defined as [43]:

$$\mu = \left[\frac{\partial E}{\partial N}\right]_V, \tag{10}$$

where V is the potential of nuclei.

Then, we might define the electronegativity: 'It is well-defined as the force of an atom in a molecule to pull electrons to itself by Pauling' as the negative of the electron chemical potential [41]:

$$X = -\mu = -\left[\frac{\partial E}{\partial N}\right]_V. \tag{11}$$

R. Mulliken indicates electronegativity as 'the average energy of the ionization and electron affinity' as follows [39]:

$$X = \frac{IP + EA}{2}. \tag{12}$$

According to Koopmans' theorem, 'it is defined as the negative val-

ue for average of the energy levels of the HOMO and LUMO' [37]:

$$X = \frac{E_{\text{HOMO}} + E_{\text{LUMO}}}{2} . \quad (13)$$

A measure of the stabilization in energy when the structure obtains the added electron charges from the environment is defined as electrophilicity [43]:

$$\omega = \kappa/(2\eta) . \quad (14)$$

3. RESULTS AND DISCUSSION

Figure 1 shows the 'optimized structure' of PVA–PEG–Yttrium ox-

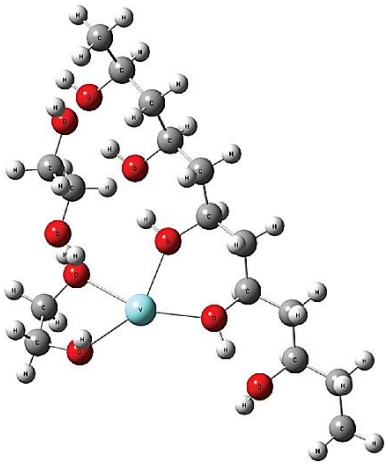

Fig. 1. Optimizing geometries of PVA–PEG–Yttrium oxide (64 atoms).

TABLE 1. Average bond lengths in [Å] and angles in [degrees].

The geometric parameters	The optimizable bonds	Values
Bonds, Å	(C–C)	1.53851
	(C–O)	1.47131
	(C–H)	1.09826
	(O–H)	1.01348
	(Y–O)	2.31069
Angles, deg.	(O–Y–O)	67.13225
	(C–C–C)	118.26195
	(C–O–H)	105.47317

ide, which obtained by the 'DFT method' with using 'three-parameter hybrid-functional' of Becke B3LYP with 6-311G basis sets.

Table 1 shows the geometric parameters of PVA–PEG–Yttrium oxide (64 atoms) including the bond length in [Ångström] and bond angle in [degrees] by the Gaussian 09-programs by using the DFT with the B3LYP/6-311G level. The calculated values of bonds in present work are in a well agreement with previous theoretical studies [44, 45].

Figure 2 and Table 2 show the results of FTIR obtained by using the Gaussian view 5.0-program and density functional theory (DFT) with 6-311G basis sets. Yttrium oxide produces variations in spectrum of PVA–PEG that comprises variation in the intensities and shift in several bonds. These changes are credited to bindings of Yt-

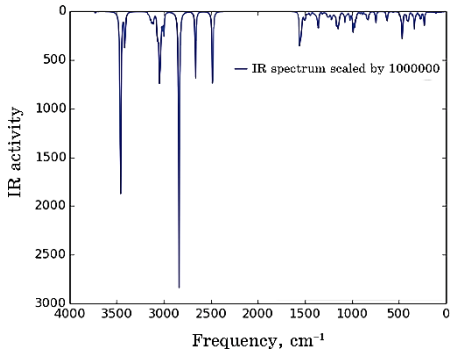

Fig. 2. IR spectrum of PVA–PEG–Yttrium oxide (64 atoms) at the B3LYP/6-311G basis set.

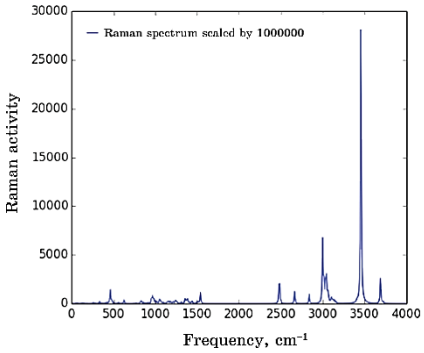

Fig. 3. Raman intensities of PVA–PEG–Yttrium oxide (64 atoms) as a function of vibrational frequency using DFT/6-311G.

TABLE 2. IR frequencies with their assignments of PVA–PEG–Yttrium oxide.

Assignment	Type of vibrational mode	Frequency, cm^{-1}	Typical vibrational frequency, cm^{-1}
Y–O	stretching	200–390	200–400 [42, 43]
C–C	stretching and bending	730–1560	700–1600 [46]
C–O	stretching	1140	1000–1280 [47]
C–O–C	bending	1250	1238–1291 [47]
$-CH_2$	in-plane bending	1355	1340–1465 [47]
C–H	symmetric stretching	3055–3046	3020–3080 [48]
O–H	stretching	3226–3631	3200–3640 [49]

trium oxide with polymers.

Figure 3 shows the Raman spectrum of PVA–PEG–Yttrium oxide (64 atoms). It is shown in this figure that the active region in IR spectrum is similar with less activity in Raman spectrum [45]. Intensities in Raman spectrum rely on probability that a particular wavelength photon will be absorbed.

Gauge-Independent Atomic Orbital (GIAO) method is used in the present NMR calculations, and chemical shifts of the structure are calculated at the same level. Absolute isotropic magnetic shielding is converted into chemical shifts by referencing to the shielding of a standard compound TMS computed at the same level. The chemical shifts are stated in p.p.m. relation to TMS for ^{1}H spectra as shown in Fig. 4.

Figure 5 shows the visible and ultraviolet spectra reliant on upon the electronic structures of the molecule. In Figure 5, absorption intensity of PVA–PEG–Yttrium oxide (64 atoms) has high UV-Vis spectra because adding the oxide leads to an increase in intensity of absorbance. As a result, this is due to moving electrons from valence level to the conduction band at these energies.

Table 3 shows the energy gap for PVA–PEG–Yttrium oxide (64 atoms). This result is in a good agreement with that in Refs. [44,

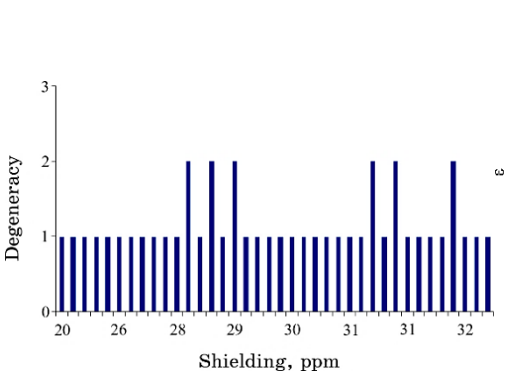

Fig. 4. Nuclear magnetic resonance of PVA–PEG–Yttrium oxide (64 atoms) in infrared spectrum as a function of vibrational frequency.

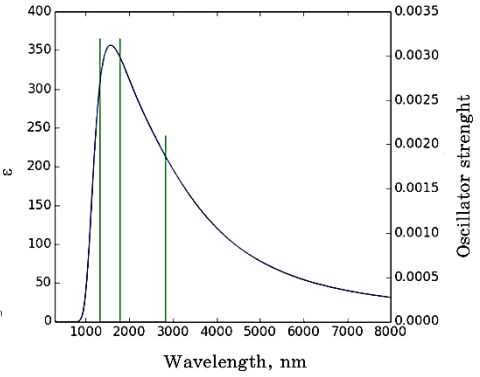

Fig. 5. UV-Vis spectrum for PVA–PEG–Yttrium oxide (64 atoms) using B3LYP/6-311G.

TABLE 3. The values of energy gap in [eV] for the studied structures.

PVA–PEG–Y_2O_3 (64 atoms)		
E_{HOMO}, eV	E_{LOMO}, eV	E_g, eV
3.02	0.008	3.028

46] and refers that PVA–PEG–Yttrium oxide needs high energy to donating or accepting an electron. Figure 6 illustrates the 3*D* distribution of HOMOs and LUMOs for the studied structures. From these results, the calculated energy gap decreases with increasing the number of atoms.

Table 4 illustrates the results for the total energy E_{tot} in [a.u.] and some electronic properties. The total ground state energy E_{tot}

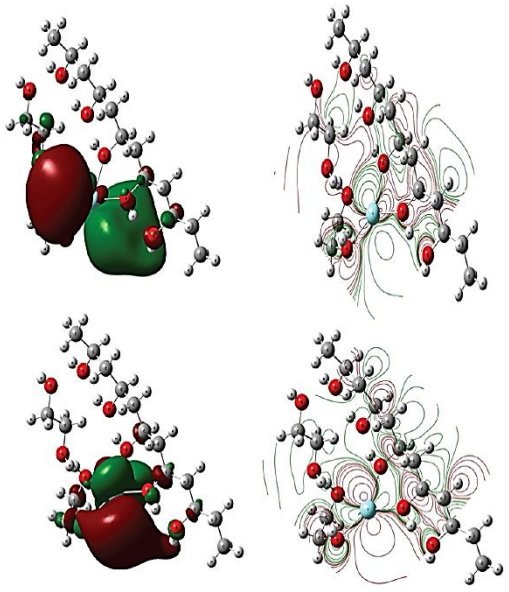

Fig. 6. The distribution of HOMO (up) and LUMO (down) for PVA–PEG–Yttrium oxide blend containing 64 atoms.

TABLE 4. The values of some electronic properties in [eV] of the studied structures.

Property	PVA–PEG–Y_2O_3 (64 atoms)
total energy	–1347.381
cohesive energy	–7.8947
ionization potential	3.02
electron affinity	0.008
electronegativity	1.514
chemical hardness	1.506
chemical softness	0.33
chemical potential	–1.514
electrophilicity	0.760
polarizability, a.u.	213.58

for PVA–PEG–Yttrium oxide is approximated by the summation of all E_{tot} for all atoms in the structure. It is identified that the frontier molecular orbitals, the high occupied molecular orbitals HOMO, and the low unoccupied molecular orbitals LUMO, show an important part for the reactant molecules in chemical reactions. It may be concluded that less negative E_{coh} value for structures might be concerned with its higher LUMO energy level because it does not need high energy to lose electrons from external orbitals. An interesting conclusion may be drawn from these investigations, namely, this factor can affect the value of cohesive energies. Here, the system with larger E_{coh} is more stable. The ionization energy I_E and electron affinity E_A for PVA–PEG–Yttrium oxide are calculated according to Koopmans' theorem. These values show that the PVA–PEG–Yttrium oxide needs to high energy to donating or accepting an electron to become cation or anion because of the high value of I_E and low value of E_A. The calculated values of electronegativity E_N and electrochemical hardness H show that structures have small capability to electron transfer. The low value of the electronic softness S is a reflection to the large separation between the valence band and conduction band. High hardness refers to high excitation energies required to electron transfer for PVA–PEG–Yttrium oxide.

In Table 4, PVA–PEG–Yttrium oxide has large absolute value of chemical potential with low value of ω. Therefore, these are weak nanocomposites to interact with other surrounding species or molecule. The nanocomposites, which have high values of polarizability, will be more effective, less stable, more softness and will have small energy gap.

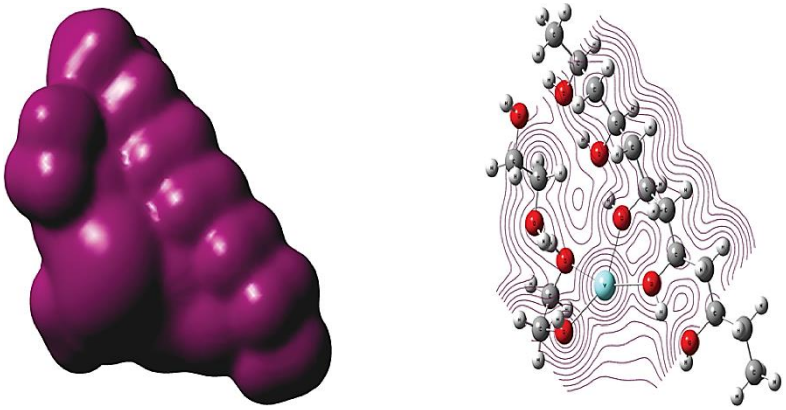

a *b*

Fig. 7. The electron density distribution for PVA–PEG–Yttrium oxide containing 64 atoms.

Figure 7 illustrates the three-dimensional shape of electron density (ED) distribution surfaces for the structures. The ED is distributed owing to distribution of all atoms in the space of the nanocomposites giving the total density of the electrons.

Figure 8 illustrates the electrostatic potential (ESP) distribution surfaces for PVA–PEG–Yttrium oxide calculated from the total self-consistent field approximation. The ESP distributions for the structures are caused by repulsive forces or by attracting regions around each nanocomposite. In general, the ESP surfaces for PVA–PEG–Yttrium oxide (64 atoms) are dragged toward the positions of

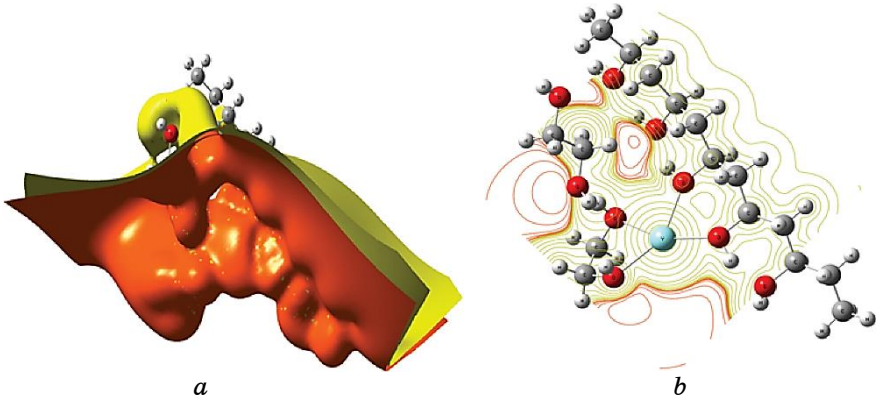

a *b*

Fig. 8. The electrostatic potential distribution surface for PVA–PEG–Yttrium oxide (64 atoms) (left: counter 2*D*; right: 3*D*).

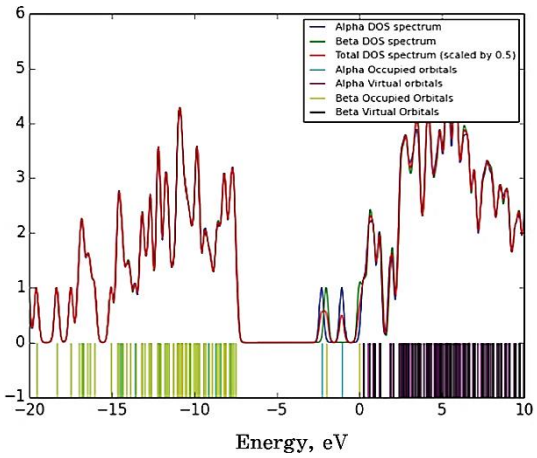

Fig. 9. Electron density of states as a function of bond length for PVA–PEG–Yttrium oxide (64 atoms).

negative charges in each molecule, which are the oxygen atoms of high electronegativity (of 3.5 eV).

Further studying the strength of the reactions can be done by analysing the orbital interactions between the PVA–PEG–Yttrium oxide blend atoms in expression for the DOS, as shown in Fig. 9. The high density of states at a specific energy level refers to the many cases in the structure available for occupations.

4. CONCLUSIONS

The B3LYP/6-311G density functional theory validity is proved in studying the geometry optimization and calculating the geometrical parameters.

Energy gap is a useful inclusive property. Soft molecules have small energy gaps and their electron density changes more easily than in hard molecules.

The ESP is dragged towards the active sites in PVA–PEG–Yttrium oxide structures.

The PVA–PEG–Yttrium oxide structures can be used for different optoelectronics applications.

REFERENCES

1. S. K. Kannan and M. Sundrarajan, *Bull. of Mater. Sci.*, **38**, No. 4: 945 (2015).
2. W. Y. Ching and Y. N. Xu, *Phys. Rev. B*, **59**, No. 20: 12815 (1999).
3. Z. Yang and S. J. Xiong, *J. of Phys. B: Atomic, Mol. and Optic. Phys.*, **42**, No. 24: 245101 (2009); https://doi.org/10.1088/0953-4075/42/24/245101
4. D. Kumar, S. K. Jat, P. K. Khanna, N. Vijayan, and S. Banerjee, *Int. J. of Green Nanotechno.*, **4**, No. 3: 408 (2012).
5. S. K. Sharma, J. Prakash, K. Sudarshan, D. Sen, S. Mazumder, and P. K. Pujari, *Macromolecules*, **48**, No. 16: 5706 (2015).
6. K. Hermann and M. Witko, *Oxide Surfaces* (Ed. D. Woodruff) (Elsevier: 2001), vol. **9**, p. 136.
7. J. Lee, D. Bhattacharyya, A. J. Easteal, and J. B. Metson, *Current Appl. Phys.*, **8**, No. 1: 42 (2008).
8. S. Ram and T. K. Mandal, *Chem. Phys.*, **303**, Nos. 1–2: 121 (2004).
9. A. Hashim, Y. Al-Khafaji, and A. Hadi, *Transactions on Elect. and Electronic Mater.*, **20**: 530 (2019); https://doi.org/10.1007/s42341-019-00145-3
10. A. Hadi, A. Hashim, and Y. Al-Khafaji, *Transactions on Elect. and Electronic Mater.*, **21**: 283 (2020); https://doi.org/10.1007/s42341-020-00189-w
11. A. Hashim, A. J. Kadham, A. Hadi, and M. A. Habeeb, *Nanosistemi, Nanomateriali, Nanotehnologii*, **19**, Iss. 2: 327 (2021); https://doi.org/10.15407/nnn.19.02.327
12. A. Hashim and Z. S. Hamad, *Nanosistemi, Nanomateriali, Nanotehnologii*, **18**, Iss. 4: 969 (2020); https://doi.org/10.15407/nnn.18.04.969

13. A. Hazim, A. Hashim, and H. M. Abduljalil, *Nanosistemi, Nanomateriali, Nanotehnologii*, **18**, Iss. 4: 983 (2020); https://doi.org/10.15407/nnn.18.04.983
14. A. Hashim, *J. of Inorganic and Organometallic Polym. and Mater.*, **30**: 3894 (2020); https://doi.org/10.1007/s10904-020-01528-3
15. A. Hashim and Z. S. Hamad, *Egypt. J. Chem.*, **63**, Iss. 2: 461 (2020); DOI: 10.21608/EJCHEM.2019.7264.1593
16. K. H. H. Al-Attiyah, A. Hashim, and S. F. Obaid, *Int. J. of Plastics Techno.*, **23**, No. 1: 39 (2019); https://doi.org/10.1007/s12588-019-09228-5
17. A. Hashim, K. H. H. Al-Attiyah, and S. F. Obaid, *Ukr. J. Phys.*, **64**, No. 2: 157 (2019); https://doi.org/10.15407/ujpe64.2.157
18. H. Ahmed, H. Abduljalil, and A. Hashim, *Transactions on Elect. and Electronic Mater.*, **20**: 218 (2019), https://doi.org/10.1007/s42341-019-00111-z
19. A. Hashim and N. Hamid, *J. of Bionanoscience*, **12**, No. 6: 788 (2018); doi:10.1166/jbns.2018.1591
20. B. Abbas and A. Hashim, *Int. J. of Emerging Trends in Eng. Res.*, **7**, No. 8: 131 (2019); https://doi.org/10.30534/ijeter/2019/06782019
21. A. Hashim and Z. S. Hamad, *J. of Bionanoscience*, **12**, No. 4: 504 (2018); doi:10.1166/jbns.2018.1561.
22. N. H. Al-Garah, F. L. Rashid, A. Hadi, and A. Hashim, *J. of Bionanoscience*, **12**, No. 3: 336 (2018); doi:10.1166/jbns.2018.1538
23. A. Hashim and A. Jassim, *Sensor Letters*, **15**, No. 12: 1003 (2017); doi:10.1166/sl.2018.3915
24. I. R. Agool, F. S. Mohammed, and A. Hashim, *Advances in Environmental Biology*, **9**, No. 11: 1 (2015).
25. F. A. Jasim, A. Hashim, A. G. Hadi, F. Lafta, S. R. Salman, and H. Ahmed, *Research Journal of Applied Sciences*, **8**, Iss. 9: 439 (2013).
26. F. A. Jasim, F. Lafta, A. Hashim, M. Ali, and A. G. Hadi, *J. of Eng. and Applied Sciences*, **8**, No. 5: 140 (2013).
27. A. Hashim, H. M. Abduljalil, and H. Ahmed, *Egypt. J. Chem.*, **62**, Iss. 9: 1659 (2019); doi:10.21608/EJCHEM.2019.7154.1590
28. A. Hashim and M. A. Habeeb, *Transactions on Elect. and Electronic Materials*, **20**: 107 (2019); doi:10.1007/s42341-018-0081-1
29. H. Ahmed, H. M. Abduljalil, and A. Hashim, *Transactions on Elect. and Electronic Mater.*, **20**: 206 (2019); https://doi.org/10.1007/s42341-019-00100-2
30. H. Ahmed, A. Hashim, and H. M. Abduljalil, *Egypt. J. Chem.*, **62**, Iss. 4: 1167 (2019); doi:10.21608/EJCHEM.2019.6241.1522
31. A. Hashim, H. M. Abduljalil, and H. Ahmed, *Egypt. J. Chem.*, **63**, Iss. 1: 71 (2020); doi:10.21608/EJCHEM.2019.10712.1695
32. H. Ahmed and A. Hashim, *Egypt. J. Chem.*, **63**, Iss. 3: 805 (2020); doi:10.21608/EJCHEM.2019.11109.1712
33. A. Hashim and Z. S. Hamad, *J. of Bionanoscience*, **12**, Iss. 4: (2018); doi:10.1166/jbns.2018.1551
34. D. Hassan and A. Hashim, *J. of Bionanoscience*, **12**, Iss. 3: (2018); doi:10.1166/jbns.2018.1537.
35. D. Hassan and A. Hashim, *J. of Bionanoscience*, **12**, Iss. 3: (2018); doi:10.1166/jbns.2018.1533.
36. H. Ahmed and A. Hashim, *Int. J. of Sci. & Techno. Res.*, **8**, Iss. 11: (2019).

37. J. Baima, A. Erba, M. Rйrat, R. Orlando, and R. Dovesi, *J. of Phys. Chem. C*, **117**, No. 24: 12864 (2013).
38. F. Jensen, *The J. of Chem. Phys.*, **116**, No. 17: 7372 (2002).
39. D. Young, *Computational Chemistry: A Practical Guide for Applying Techniques to Real World Problems* (John Wiley & Sons Inc: 2001); DOI:10.1002/0471220655
40. H. W. Hugosson, *A Theoretical Treatise on the Electronic Structure of Designer Hard Materials* (Doctoral dissertation) (Acta Universitatis Upsaliensis: 2001).
41. W. J. Hehre, L. Radom, P. R. Schleyer, and J. A. Pople, *Ab initio Molecular Orbital Theory* (New York: John Wiley & Sons Inc.: 1986).
42. M. Oftadeh, S. Naseh, and M. Hamadanian, *Comp. and Theor. Chem.*, **966**: Nos. 1–3: 20 (2011).
43. K. Sadasivam and R. Kumaresan, *Comp. and Theor. Chem.*, **963**, No. 1: 227 (2011).
44. A. B. Rahane, P. A. Murkute, M. D. Deshpande, and V. Kumar, *J. of Phys. Chem. A*, **117**, No. 26: 5542 (2013).
45. B. Dai, K. Deng, and J. Yang, *Chem. Phys. Letters*, **364**, Nos. 1–2: 188 (2002).
46. T. Larbi, K. E. El-Kelany, K. Doll, and M. Amlouk, *J. of Raman Spectroscopy*, **51**, No. 2: 232 (2020).
47. H. K. Lin, C. B. Wang, H. C. Chiu, and S. H. Chien, *Catalysis Letters*, **86**, Nos. 1–3: 63 (2003).
48. P. Atkins and J. De Paula, *Physical Chemistry for the Life Sciences* (Oxford, USA: Oxford University Press: 2011).
49. E. Kavitha, N. Sundaraganesan, and S. Sebastian, *Indian J. of Pure and Appl. Phys.*, **48**, No. 1: 20 (2010).